Bixin, an apocarotenoid isolated from Bixa orellana L., sensitizes human melanoma cells to dacarbazine-induced apoptosis through ROS-mediated cytotoxicity

Raimundo Gonçalves de Oliveira Júnior, Antoine Bonnet, Estelle Braconnier, Hugo Groult, Grégoire Prunier, Laureen Beaugeard, Raphäel Grougnet, Jackson Roberto Guedes da Silva Almeida, Christiane Adrielly Alves Ferraz, Laurent Picot

Bixin, an apocarotenoid isolated from *Bixa orellana* L., sensitizes human melanoma cells to dacarbazine-induced apoptosis through ROS-mediated cytotoxicity

Raimundo Gonçalves de Oliveira Júnior[a], Antoine Bonnet[a,b], Estelle Braconnier[a], Hugo Groult[a], Grégoire Prunier[a], Laureen Beaugeard[a], Raphäel Grougnet[c], Jackson Roberto Guedes da Silva Almeida[d], Christiane Adrielly Alves Ferraz[d], Laurent Picot[a]

[a]*UMRi CNRS 7266 LIENSs, Université de La Rochelle, 17042 La Rochelle, France.*

[b]*Plateforme d'analyse haute résolution des biomolécules, UMR CNRS 7266 LIENSs, 17042 La Rochelle, France.*

[c]*UMR CNRS 8638 Laboratoire de Pharmacognosie, Universté Paris Descartes, 75006 Paris, France.*

[d]*Núcleo de Estudos e Pesquisas de Plantas Medicinais, Universidade Federal do Vale do São Francisco, 56306-000 Petrolina, Brazil.*

*Corresponding author at: UMRi CNRS 7266 LIENSs, Université de La Rochelle, Curie B101 Faculté des Sciences et Technologies, Avenue Michel Crépeau, 17042 La Rochelle, France. E-mail address: laurent.picot@univ-lr.fr (Laurent Picot).

ABSTRACT

Cutaneous melanoma has a high capacity to metastasize and significant resistance to conventional therapeutic protocols, which makes its treatment difficult. The combination of conventional drugs with cytostatic molecules of low toxicity has been shown to be an interesting alternative for sensitization of tumor cells to chemotherapy. In this study, we evaluated the effect of bixin, an abundant apocarotenoid present in *Bixa orellana*, on the sensitization of human melanoma cells (A2058) to dacarbazine treatment, an anticancer agent clinically used for the therapy of metastatic melanoma. UPLC-DAD-MS/MS analyses of bioactive extracts from *B. orellana* seeds led to the identification of two new apocarotenoids: 6,8'-diapocarotene-6,8'-dioic acid and 6,7'-diapocarotene-6,7'-dioic acid. After being identified as its major compound, bixin (*Z*-bixin) was evaluated on A2058 cells expressing the oncogenic BRAF VE600 mutation and resistant to dacarbazine treatment. Bixin promoted growth inhibition, reduced cell migration, induced apoptosis and cell cycle arrest in the G2/M phase. When associated with dacarbazine, bixin restored the sensitivity of A2058 cells to chemotherapy, enhancing its antiproliferative, anti-migratory and pro-apoptotic effects. Combined treatment also induced higher ROS (reactive oxygen species) and MDA (malondialdehyde, a lipid peroxidation marker) generation than monotreatment, suggesting that the oxidative stress caused by bixin contributes significantly to its sensitizing effect. Taken together, these data suggest that bixin exerts intrinsic antimelanoma activity by mechanisms complementary to those of dacarbazine, encouraging its use in combined therapy for cutaneous melanoma treatment.

Keywords: annatto, dacarbazine, carotenoids, melanoma, multidrug resistance.

Highlights

- Identification of two new apocarotenoids (6,8'-diapocarotene-6,8'-dioic acid and 6,7'-diapocarotene-6,7'-dioic acid).
- First detection of naringenin and β-12'-apo-carotenoic acid in *B. orellana*.
- Purification, characterization and pharmacological evaluation of bixin (*Z*-bixin) on human melanoma cells.
- Sensitization of melanoma cells to dacarbazine treatment by bixin (combined therapy).
- Potentialization of pro-apoptotic effect of dacarbazine by increasing oxidative stress.

1. Introduction

Although it has a low incidence, melanoma is responsible for about 80% of skin cancer-associated mortality (MacKie et al., 2009). It has a high propensity to metastasize and is poorly responsive to most of the conventional therapies. In general, metastatic melanoma presents a dismal prognosis, with a five-year overall survival rate of only 15% and a median survival of less than eight months with treatment (Chakraborty et al., 2013; Locatelli et al., 2013).

In recent years, limited progress has been achieved in the treatment of metastatic melanoma through immunotherapy and target therapy (Flaherty and McArthur, 2010; Sosman and Puzanov, 2006). In 2011, the Food and Drug Administration (FDA) approved vemurafenib (BRAF inhibitor) and ipilimumab (monoclonal antibody) for clinical trials in patients with metastatic melanoma. Melanoma therapy may also include the use of alkylating agents (e.g., dacarbazine, temozolomide), platinum derivatives (e.g., cisplatin, carboplatin), vinca alkaloids (e.g., vindesine, vinblastine) and cytokines (e.g., IFN-α, IL-2) (Bhatia et al., 2009; Chapman et al., 2011; Jin et al., 2018; Locatelli et al., 2013). However, melanoma cells display multidrug resistance (MDR) mechanisms, which requires the use of higher doses to ensure a satisfactory pharmacological response. Unsuccessful treatments are often attributed to alterations in drug metabolism, efflux pump expression, apoptosis evasion mechanisms and mutations in specific therapeutic targets (Tentori et al., 2013).

To improve therapeutic response, several combinations of anticancer drugs with different mechanisms of action have been studied (Jin et al., 2018). Many combinatorial treatments tested in melanoma have associated immunologic agents (e.g., IFN-α, IL-2), hormones (e.g., tamoxifen) and target therapy drugs (e.g., vemurafenib) with dacarbazine, an alkylating agent considered as a single drug reference for the management of advanced melanoma. Nevertheless, the toxicity of these combinatorial treatments has been a limiting factor and no survival benefit has been demonstrated in comparison to monotherapy (Garbe et al., 2008; Mouawad et al., 2010).

A variety of natural products has been reported for cancer therapy, acting not only as chemotherapeutic or chemopreventive agents but also by enhancing the effectiveness of conventional chemotherapy (Vinod et al., 2013). Natural molecules sensitize tumor cells to chemotherapy by increasing the residence time of anticancer drugs in the cell, disrupting the cellular cytoskeleton, promoting DNA damage, inducing apoptosis, and/or regulating the expression of altered molecular targets (de Oliveira Júnior et al., 2018; Juin et al., 2018). In

addition, natural products generally show a better tolerance profile compared to conventional therapy, have lower toxicity and promote fewer side effects.

Bixa orellana L. is a Brazilian medicinal plant, popularly known as "urucum" and "colorau" (in Brazil), “achiote” (in Mexico), and "annatto" (in the USA). *B. orellana* has economic importance mainly due to its seeds, which provide a red dye widely used in food products, textile, pharmaceutical and cosmetic industries. In fact, about 70% of all natural coloring agents consumed worldwide are derived from annatto. In traditional medicine, its seeds are commonly used to treat diabetes, diarrhea, hepatitis and dyslipidemia. Previous pharmacological investigations showed that *B. orellana* seeds have antimicrobial, anti-inflammatory, antioxidant, hypoglycemic and cytotoxic effects (Shahid-ul-Islam et al., 2016; Vilar et al., 2014). The therapeutic properties and industrial applications of annatto seeds are directly related to the carotenoid content, especially bixin, the major apocarotenoid of this species (Priya et al., 2017; Rivera-Madrid et al., 2016). In *in vitro* studies, bixin exhibited anticancer activity against HL60 (leukemia), B16 (melanoma), U20S (osteosarcoma), PC3 (prostate), HCT-116 (colon), MCF-7 (breast), DRO (anaplastic thyroid) and BHP-16 (papillary thyroid) cell lines. Bixin inhibited the proliferation of tumor cells in a concentration-dependent manner, through apoptosis induction and cell cycle arrest (Anantharaman et al., 2016; Santos et al., 2016; Tibodeau et al., 2010). Interestingly, this metabolite has shown low toxicity in animal models (Agner et al., 2004; Bautista et al., 2004; Paumgartten et al., 2002; Stohs, 2014), and it is therefore considered as a good candidate for sensitizing tumor cells.

In this present report, we described additional outcomes on the molecular mechanisms involved in the bixin pro-apoptotic effect and assessed its ability to sensitize melanoma cells to dacarbazine. All experiments were performed using the highly invasive A2058 human melanoma cell line, expressing the V600E BRAF oncogenic mutation, and resistant to dacarbazine therapy.

2. Materials and Methods

2.1. Plant material

Seeds of *Bixa orellana* were collected in Missão Velha (Coordinates: S 07°14’59”, W 39°08’35”), State of Ceará, Brazil, in August 2017. Botanical identification was performed by comparison with a voucher specimen previously deposited at the Herbário Vale do São Francisco of the Universidade Federal do Vale do São Francisco (n° 16750). Once collected,

botanical material was dried in an oven (40 °C) with air circulation, for 72 hours. All procedures for access to genetic patrimony and associated traditional knowledge were carried out and the project was registered in SisGen (Register #A45AFE5).

2.2. Extraction

Dried seeds (46 g) were submitted to sequential maceration using hexane (2.0 L), chloroform (2.0 L), ethyl acetate (2.0 L) and methanol (2.0 L) in increasing polarity order. Two hours were designed for each extraction solvent, employing constant stirring (1000 rpm) at 50 °C. Extractive solutions were filtrated and concentrated on a rotatory evaporator at a maximum temperature of 50 °C, resulting in hexane (Hex-Bo, 4.68 g), chloroform ($CHCl_3$-Bo, 1.88 g), ethyl acetate (EtOAc-Bo, 0.045 g) and methanol (MeOH-Bo, 0.22 g) extracts. All extracts were stored at -20 °C until chemical analysis and cell viability assay.

2.3. UPLC-DAD-MS/MS analysis

Analyses were carried out using an UHPLC system "Acquity UPLC H-class" (Waters, Milford, USA) coupled to a photodiode array (Waters 2996) and a high resolution mass spectrometer "XEVO G2S Q-TOF" equipped with an electrospray ionization source (Waters, Manchester, England). The UHPLC system was formed by a quaternary pump (Quaternary Solvent Manager, Waters) and an automatic injector (Sample Manager-FTN, Waters) equipped with a 10 μL injection loop. 5 μL of the samples were injected in a column "Acquity UPLC BEH C18" (Waters) (2.1 × 50 mm, 1.7 μm), and the products were eluted at a flow rate of 300 $\mu L.min^{-1}$ using a gradient composed of solvents A (water/formic acid 100/0.001 (v:v)) and B (methanol/ formic acid 100/0.001 (v:v)), according to the following procedure: 0–1 min, 10% B; 1–2.5 min 10%–50% B ; 2.5–7 min 50% B; 7–10 min 50–30% B; 10–12 min, 30%-25% B; 12-15 min 25% B; 15-17 min 25%-20% B; 17-20 min 20% B; 20-23 min 20%-17% B; 23-26 min 17% B; 26-28 min 17-15% B; 28-31 min 15% B; 31-32 min 15-10% B; 32-35 min 10% B; 35-36 min 90%-10% B; 36-39 min 10% B. During the analysis, the column and the injector were maintained at 25 °C and 7 °C, respectively. The instrument was adjusted for the acquisition on a 250–800 nm interval in UV mode, with 5 $spectra.s^{-1}$ and 1.2 nm of resolution. The analyses were performed in positive ionization mode with MSE function in a centroid mode. The MS parameters was applied in the ESI source for the two ionization mode were: source temperature 120 °C, desolvation temperature 500 °C, gas flow-rate of the cone 50 $L.h^{-1}$, desolvation gas flow-rate 800 $L.h^{-1}$, capillary voltage 3.0 kV, sampling cone 130 V and source compensation 80 V. The instrument was adjusted for the

acquisition on a 250–1300 m/z interval, with a scan time of 0.15 s. The mass spectrometer was calibrated before analysis using 0.5 mM sodium formate solution, and Leucine Enkephalin (M = 555.62 Da,1 ng. μL^{-1}) was used as a lock-mass.

2.4. Isolation and characterization of bixin

After extraction, hexane extract showed a red precipitate. The supernatant was separated and the precipitate was washed successively in methanol, leading to isolation of bixin (1.15 g). The chemical characterization and purity of the sample were determined by UPLC-DAD-MS/MS analysis, as described in the previous topic. To ensure complete structural elucidation, ^{1}H and ^{13}C NMR experiments were performed on a JEOL JNM-LA400 spectrometer (Croissy-sur-Seine, France) operating at 400 MHz for ^{1}H experiment, 100 MHz for ^{13}C experiment. NMR spectra were obtained in deuterated DMSO (DMSO-d_6), using tetramethylsilane as an internal standard, with chemical shifts expressed in ppm (δ) and coupling constants (*J*) in Hz. Proton-coupling patterns were described as singlet (s), doublet (d), triplet (t), or multiplet (m).

2.5. Cell line and culture conditions

A2058 (ATCC® CRL-11147™, LGC ATCC Standards, France) is a melanoma cell line obtained from metastatic cells removed from lymph nodes of a 43-year-old caucasian patient. Due to its highly invasive, metastatic and chemoresistance potentials related to V600E mutation in BRAF and mutations in PTEN and P53 genes, A2058 provides a clinically relevant model for evaluation not only of new anti-melanoma molecules, but also of new chemosensitizer agents, allowing the assessment of combined therapy (Dankort et al., 2009; Juin et al., 2018). Cells were grown in 75 cm² flasks using DMEM (Dutscher, France) supplemented with 10% FCS (Dutscher, France) and 1% penicillin-streptomycin (1000 $U.ml^{-1}$ and 100 $\mu g.ml^{-1}$, respectively) (Dutscher, France), at 37 °C in a 5% CO_2 humidified atmosphere.

2.6. Cell viability assay

The antiproliferative activity of extracts (Hex-Bo, $CHCl_3$-Bo, EtOAc-Bo and MeOH-Bo) and bixin was determined using the MTT (Sigma-Aldrich®, France) assay (Juin et al., 2018; Mosmann, 1983). Cells (2 x 10^3/well) were grown in 96-well plates with extracts (100 $\mu g.ml^{-1}$) or increasing concentrations of bixin (0.1-100 µM). Cells were also exposed to varying concentrations of vemurafenib (0.1-100 µM) and dacarbazine (0.1-100 µM), alone or combined to bixin (0.1-100 µM) to assess its sensitizing effect. After 72h of treatment, 20 µl

of a MTT solution (5 $g.L^{-1}$) was added to each well and microplates were again incubated for 4h. Subsequently, the cell culture medium was removed and formazan crystals were dissolved in 100 µl DMSO. Absorbance was read at 550 nm using FLUOstar Omega microplate reader (BMG Labtech, France) and then converted into cell growth inhibition (GI%). Cellular morphology was observed after treatments under inverted phase contrast microscope (Nikon, Eclipse, France). IC_{50} was determined by nonlinear regression analysis using Prism 6.0 (GraphPad Software).

2.7. Cell migration assay

Cells (2 x 10^4/well) were incubated and grown to 90% confluence in 24-well plates. Cell monolayers were scratched with a sterile plastic tip, washed with PBS and incubated in a new cell culture medium containing bixin (50 and 100 µM), dacarbazine (50 and 100 µM) or combined treatment, for 24h. Cell migration was microscopically (100x) monitored at 0 and 24h (Cisilotto et al., 2018). Results were expressed as percentage of cell migration calculated by measuring the cell surface using ImageJ software.

2.8. Apoptosis analysis

2.8.1. Annexin V-Cy3 and 6-CFDA detection assay

Apoptosis was evaluated by using double staining with annexin V-Cy3 (red) and 6-carboxyfluorescein diacetate (6-CFDA, green) (Sigma-Aldrich®, France). Cells (5 x 10^3/well) were incubated in culture conditions for 24h, and then treated with bixin (50 and 100 µM), dacarbazine (50 µM) or both (bixin 50 µM + dacarbazine 50 µM) for 72h. Cells were further washed with PBS, suspended in binding buffer and stained with Annexin V and 6-CFDA solution for 10 min, according to manufacturer's recommendations. DAPI solution was also added to the wells for DNA labelling of necrotic cells (Juin et al., 2018). Cells treated with Staurosporine 1 µM for 4h were used as a positive control. Finally, cells were observed under fluorescent microscope (ZEISS Axion Observer, France).

2.8.2. Caspase-3 colorimetric assay

Caspase-3 activity was determined using a colorimetric assay (CASP3C kit, Sigma-Aldrich®, France) based on the hydrolysis of the peptide substrate acetyl-Asp-Glu-Val-Asp p-nitroanilide (Ac-DEVD-pNA), resulting in the release of p-nitroanilide (pNA) (Juin et al., 2018). Cell suspension (2.5 ml at 5 x 10^5 $cell.ml^{-1}$) was added to 75 cm^2 flasks containing 12.5

ml of cell culture medium (control group), bixin (50 µM), dacarbazine (50 µM) or combined drugs (bixin 50 µM + dacarbazine 50 µM) solubilized in cell culture medium. After 72h of treatment, cells were washed with PBS, lysed with lysis buffer, and caspase-3 activity was measured according to manufacturer's protocol. Results were expressed as µmol pNA/min/ml. Cells treated with Staurosporine 1 µM for 4h were used as a positive control.

2.9. Oxidative stress analysis

2.9.1. Determination of ROS levels

Fluorescence microscopy imaging was used to investigate qualitative ROS generation in A2058 cells. Cells (5 x 10^3/well) were incubated in culture conditions for 24h, and then exposed to bixin (50 µM), dacarbazine (50 µM) and combined drugs for 24h. After treatment, cells were washed with PBS and incubated with 2,7-dichlorodihydrofluorescein diacetate (DCFH-DA, 20 µM) solution for 30 min at 37 °C. The reaction mixture was removed and replaced by 200 µl of PBS in each well. An inverted fluorescent microscope (ZEISS Axio Observer, France) was used to visualize intracellular fluorescence (green) of cells and to capture images.

For quantitative ROS analysis, cells (4 x 10^3/well) were seeded in 96-well black bottom culture plate and allowed to adhere for 24h in culture conditions. Then, cells were treated with bixin (50 µM), dacarbazine (50 µM) or combined drugs for 24h. Subsequently, culture medium was discarded and cells were washed in PBS before incubation with DCFH-DA 20 µM solution for 45 min at 37 °C. Fluorescence intensity was measured in FLUOstar Omega microplate reader at excitation wavelength of 480 nm and emission wavelength of 520 nm. Values were expressed as the percentage of fluorescence intensity relative to the control group (untreated cells) (Ahamad et al., 2014).

2.9.2. Determination of MDA levels

Lipid peroxidation was determined by the reaction of malondialdehyde (MDA), an important marker for oxidative stress (Grotto et al., 2009), with thiobarbituric acid (TBA) to form a colorimetric product (532 nm), proportional to the MDA present (Lipid Peroxidation MDA assay kit, Sigma-Aldrich®, France). Cells (2.5 ml at 5 x 10^5 cell.ml^{-1}) were grown in 75 cm^2 flasks to adhere for 24h. Then, cells were treated with bixin (50 µM), dacarbazine (50 µM) or combined drugs for 24h. After treatments, cells were washed and suspended in PBS. Cell suspensions were diluted in PBS to obtain standardized concentrations of 1 x 10^6 cell.ml^{-1}

for all groups. Subsequently, cells were lysed for MDA extraction and quantification according to manufacturer's recommendations.

2.10. Cell cycle analysis

A2058 cells were grown in control culture medium or treated with bixin 50 µM, dacarbazine 50 µM or combined therapy (dacarbazine + bixin) for 72h before being stained for 30 min at 37°C in PBS containing propidium iodide (PI 100 $\mu g.ml^{-1}$), Rnase A (100 $\mu g.ml^{-1}$) and 0.1% Triton X-100 (ThermoFisher Scientific, France). Cells were analyzed using a FACS Cantoll flux cytometer (BD Biosciences, France) equipped with an air cooled blue LASER (λ=488 nm, 20 mW). Light diffusion parameters (forward and lateral scatter lights) were optimized to define the size threshold excluding cellular debris and cell clusters for single-cell fluorescence analysis. PI fluorescence was measured using a FL3 filter (λ= 670 nm) and analyzed using the BD FACS Diva Software (BD Biosciences, France). Distribution of A2058 cells in the different cell cycle phases was determined according to their DNA content as measured by the fluorescence intensity of PI: diploid cells (2n): G0/G1 phase; replicative cells (2n<DNA content<4n): S phase; tetraploid cells (4n): G2/M phase; hypodiploid cells (DNA content < 2n): apoptotic sub-G1 phase (Juin et al., 2018).

2.11. Statistical analysis

Data were expressed as mean ± SEM from three independent experiments. Unpaired Student's t and one-way ANOVA followed by Tukey's multiple comparison tests were performed according to the case (statistical significance when $p<0.05$), using Prism 6.0 (GraphPad software).

3. Results and discussion

3.1. Chemical composition of bioactive B. orellana extracts

Initially, the antiproliferative effect of all extracts was determined using the MTT assay. Hex-Bo, $CHCl_3$-Bo and EtOAc-Bo presented high antiproliferative activity at 100 $\mu g.ml^{-1}$ (Table 1). MeOH-Bo was considered inactive against A2058 cells. Subsequently, the chemical characterization of bioactive extracts was performed by UPLC-DAD-MS/MS analysis.

Table 1. Antiproliferative activity (AA) of *B. orellana* extracts (100 µg.ml^{-1}) against A2058 cells.

Extract	Hex-Bo	$CHCl_3$-Bo	EtOAc-Bo	MeOH-Bo
AA (%)	96.11 ± 3.43	93.26 ± 3.24	84.54 ± 3.16	12.03 ± 2.30

Results are expressed as mean ± SEM from at least three independent experiments.

UPLC-DAD has provide a chromatogram containing thirteen major peaks (Fig. 1). Among the identified compounds, *Z*-bixin (**8**) was the major chemical constituent in all extracts, in agreement with previous reports (Shahid-ul-Islam et al., 2016; Vilar et al., 2014). Bixin derivatives (norbixin and methyl-bixin) have also been identified (Jondiko and Pattenden, 1989). In fact, bixin is the main apocarotenoid detected in *B. orellana* seeds, and the presence of its derivatives and isomers has been exhaustively reported in the literature, as well as their chromatographic profiles, which allowed us to determine them unambiguously in the analyzed extracts (Mercadante et al., 1997; Rehbein et al., 2007; Tocchini and Mercadante, 2001). Other compounds already described for this plant were also identified, such as geranylgeraniol (**9**), δ-tocotrienol (**12**), γ-tocotrienol (**13**) and eicosatrienoic acid (**4**) (Jondiko and Pattenden, 1989). Moreover, we also manage to identify two compounds previously undescribed in *B. orellana*: naringenin (**1**) and β-12'-apo-carotenoic acid (**11**). To date, only three flavonoids have been reported for this species (leucocyanidin, luteolin and apigenin) (Chisté et al., 2011; Shahid-ul-Islam et al., 2016). In addition to contribute to its chemical knowledge, the identification of the flavonoid naringenin demonstrates that our analytical method may be employed for the simultaneous analysis of carotenoids and phenolic compounds in *B. orellana* extracts (Figs. 1, 2 and 3, Table 2).

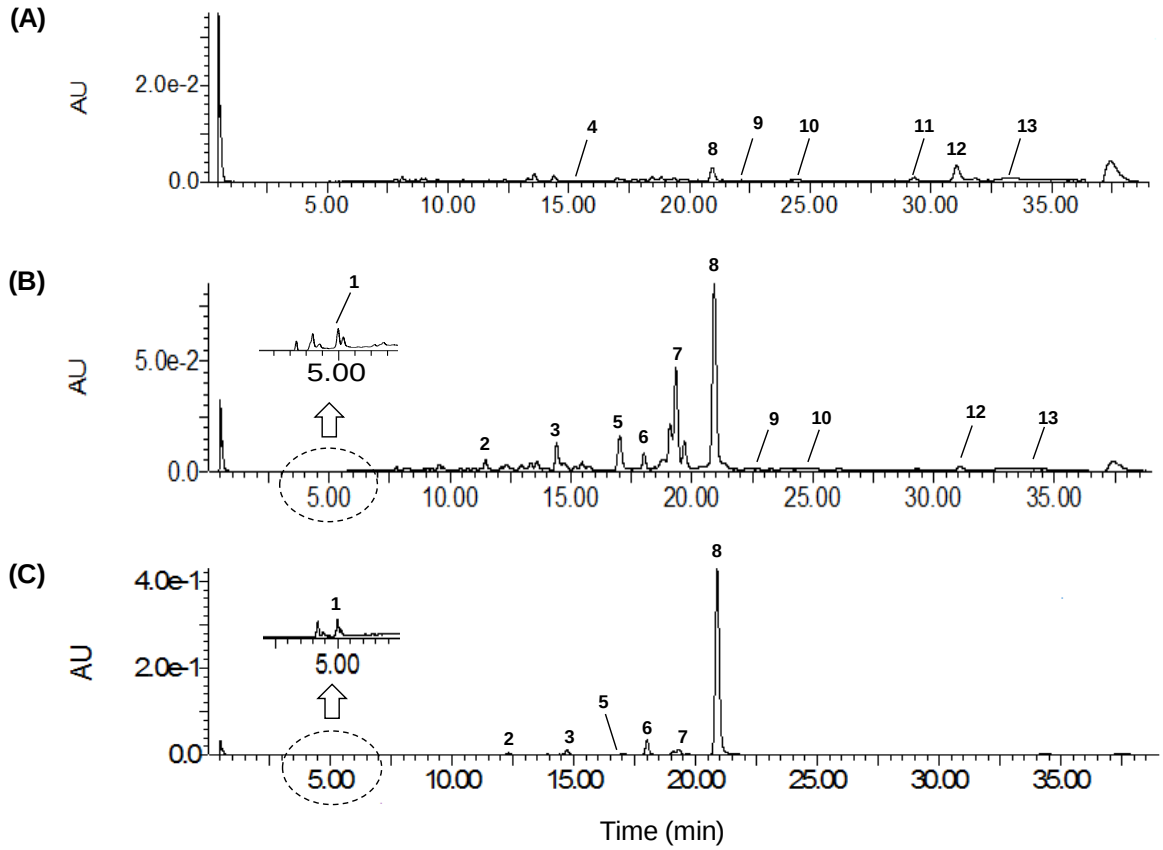

Fig. 1. UPLC-DAD chromatograms of Hex-Bo (A), $CHCl_3$-Bo (B) and EtOAc-Bo (C) at 460 nm. Figure inset was processed at 320 nm. Peak characterization is given in table 2.

Interestingly, UPLC-DAD-MS/MS analysis also showed the presence of two unpublished compounds. Compounds **2** and **5** presented a characteristic UV absorption profile for apocarotenoids, with λ_{max} at around 420, 445 and 475 nm (Table 2). The ions *m/z* 355.1906 and 369.2057 $[M+H]^+$, 377.1729 and 391.1878 $[M+Na]^+$, allowed to establish the molecular formulas $C_{22}H_{26}O_4$ and $C_{23}H_{28}O_4$ for each compound, respectively. The structures of **2** and **5** were proposed after fragmentation study (Fig. 4). All fragments present experimental mass consistent with theoretical values. In addition, some analogues of these molecules have been described in *B. orellana* extracts, suggesting that **2** and **5** can occur from known biosynthetic pathways (Mercadante et al., 1997; Rivera-Madrid et al., 2016). All these data led to the identification for **2** and **5** as the original following structures: 6,8'-diapocarotene-6,8'-dioic and 6,7'-diapocarotene-6,7'-dioic acids, respectively.

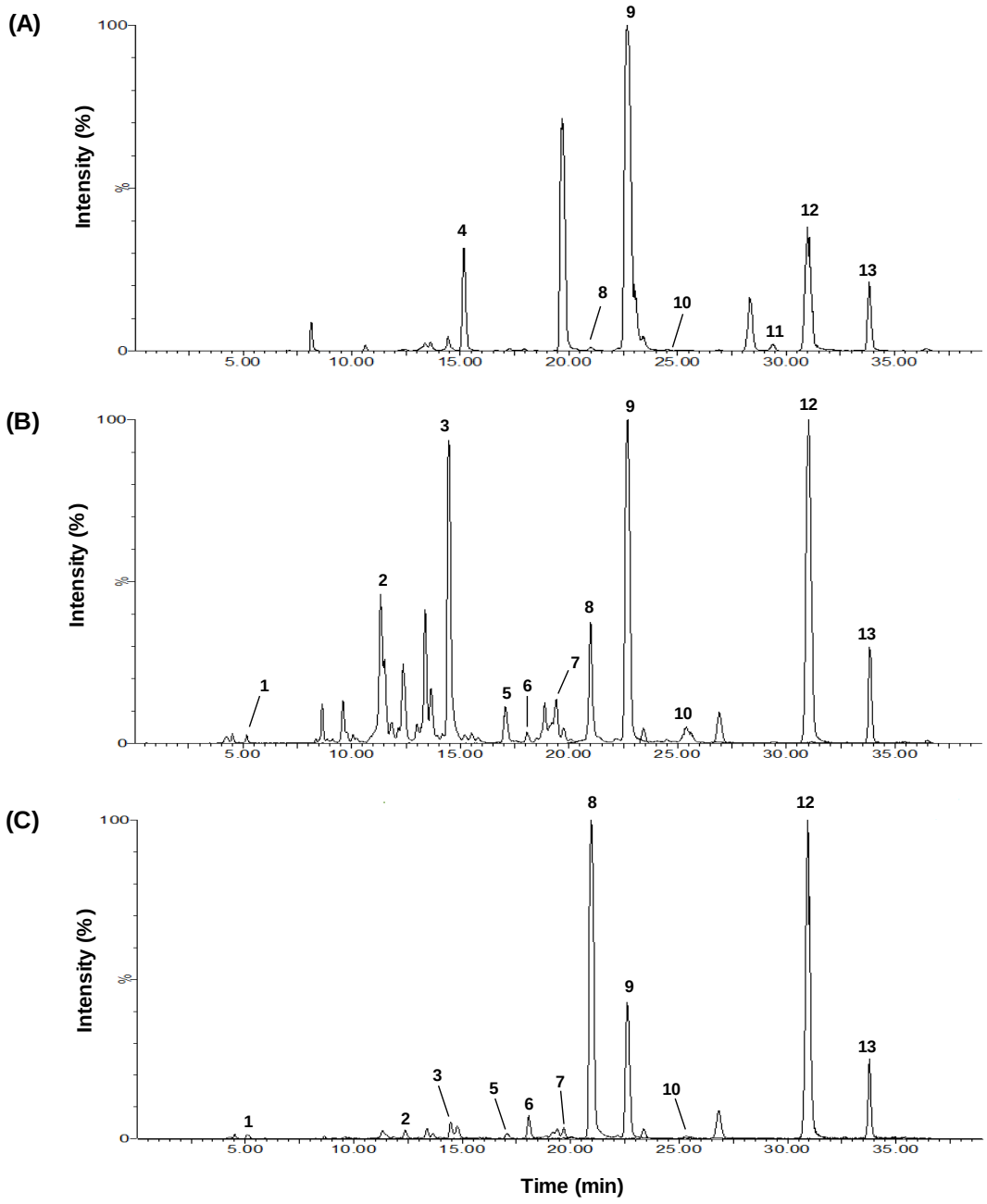

Fig. 2. Total ion chromatograms (TICs) of Hex-Bo (A), $CHCl_3$-Bo (B) and EtOAc-Bo (C), in positive mode ionization. Peak characterization is given in table 2.

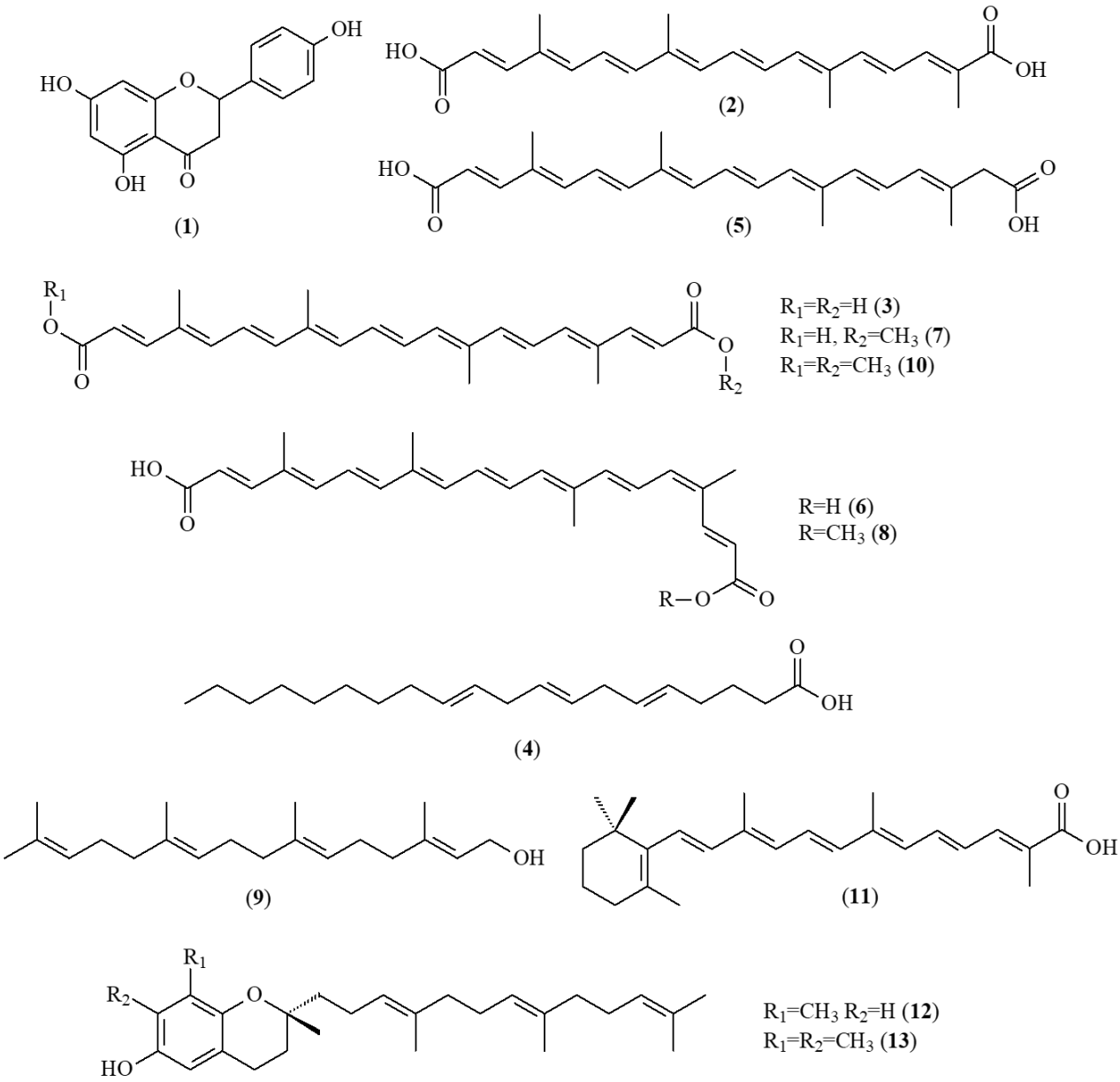

Fig. 3. Chemical structure of compounds identified in *B. orellana* extracts. Compound number is in accordance with peak number presented in Figs. 1 and 2, and Table 1.

Table 2. Identified compounds in *B. orellana* extracts by UPLC-DAD-MS/MS analysis. Peak number according to Figs. 1 and 2.

Peak	Compound	t_R (min)	Molecular formula	λ_{max} (nm)	Experimental *m/z* (Δ, ppm)			MS^2 fragments *m/z*
					$M^{\cdot+}$	$[M+H]^+$	$[M+Na]^+$	
1	Naringenin	4.99	$C_{15}H_{12}O_5$	290, 321		273.0759 (1.4 ppm)		153.0182, 147.0440
2	6,8'-diapocarotene-6,8'-dioic acid	11.34	$C_{22}H_{26}O_4$	422, 448, 472		355.1906 (0.8 ppm)	377.1729 (0.0 ppm)	337.1802, 319.1695, 277.1592, 256.1455, 225.1274, 145.1009
3	*E*-norbixin	14.79	$C_{24}H_{28}O_4$	432, 453, 484		381.2060 (1.6 ppm)	403.1884 (0.2 ppm)	349.1793, 321.1845, 283.1677, 251.1430, 217.1232
4	Eicosatrienoic acid	15.37	$C_{20}H_{34}O_2$	-		307.2634 (1 ppm)	329.2457 (0.3 ppm)	289.2528, 271.2423, 261.2576, 247.2057, 231.2115, 135.1166
5	6,7'-diapocarotene-6,7'-dioic acid	17.05	$C_{23}H_{28}O_4$	425, 445, 478		369.2057 (2.4 ppm)	391.1878 (1.8 ppm)	351.1952, 337.1797, 319.1690, 309.1848, 291.1743, 277.1584, 255.1379, 225.1275, 209.1327, 157.1011, 145.1008
6	*Z*-norbixin	18.07	$C_{24}H_{28}O_4$	430, 460, 485		381.2064 (0.5 ppm)	403.1890 (1.2 ppm)	363.1952, 345.1848, 335.2005, 317.1902, 282.1616
7	*E*-bixin	19.31	$C_{25}H_{30}O_4$	430, 455, 485	394.2141 (0.8 ppm)	395.2216 (1.5 ppm)	417.2043 (0.2 ppm)	377.2105, 363.1952, 345.1850, 335.2004, 317.1900,289, 1954 282.1609, 209.1324, 157.1011, 145.1011
8	*Z*-bixin	20.95	$C_{25}H_{30}O_4$	430, 461, 490	394.2142 (0.8 ppm)	395.2227 (1.3 ppm)	417.2043 (0.2 ppm)	377.2103, 363.1950, 345.1840, 335.1996, 317.1903, 289.1942, 282.1600, 209.1322, 157.1010, 145.1011
9	Geranylgeraniol	22.78	$C_{20}H_{34}O$	-		291.2682 (2.0 ppm)	313.2510 (1.0 ppm)	273.2581, 233.2265, 217.1953, 191.1781, 177.1638, 163.1489, 149.1310, 135.1173, 123.1163,

								109.1012, 95.0859
10	Methyl-bixin	24.50	$C_{26}H_{32}O_4$	432, 452, 482	408.2297 (1.0 ppm)	409.2351 (6.8 ppm)	431.2199 (0.2 ppm)	393.2072, 377.2113, 349.2157, 317.1895, 289.1946
11	β-12’-apo-carotenoic acid	29.41	$C_{25}H_{34}O_2$	395	366.2556 (0.8 ppm)	367.2631 (1.6 ppm)	389.2458 (0.5 ppm)	349.2513, 297.1849, 268.2185, 243.1380, 225.1275, 199.1478
12	δ-tocotrienol	31.02	$C_{27}H_{40}O_2$	296		397.3097 (2.5 ppm)	419.2924 (0.5 ppm)	191.1064, 177.0912, 137.0592,
13	γ-tocotrienol	33.82	$C_{28}H_{42}O_2$	297		411.3248 (3.6 ppm)	433.3078 (1.1 ppm)	205.1220, 191.1063, 151.0748

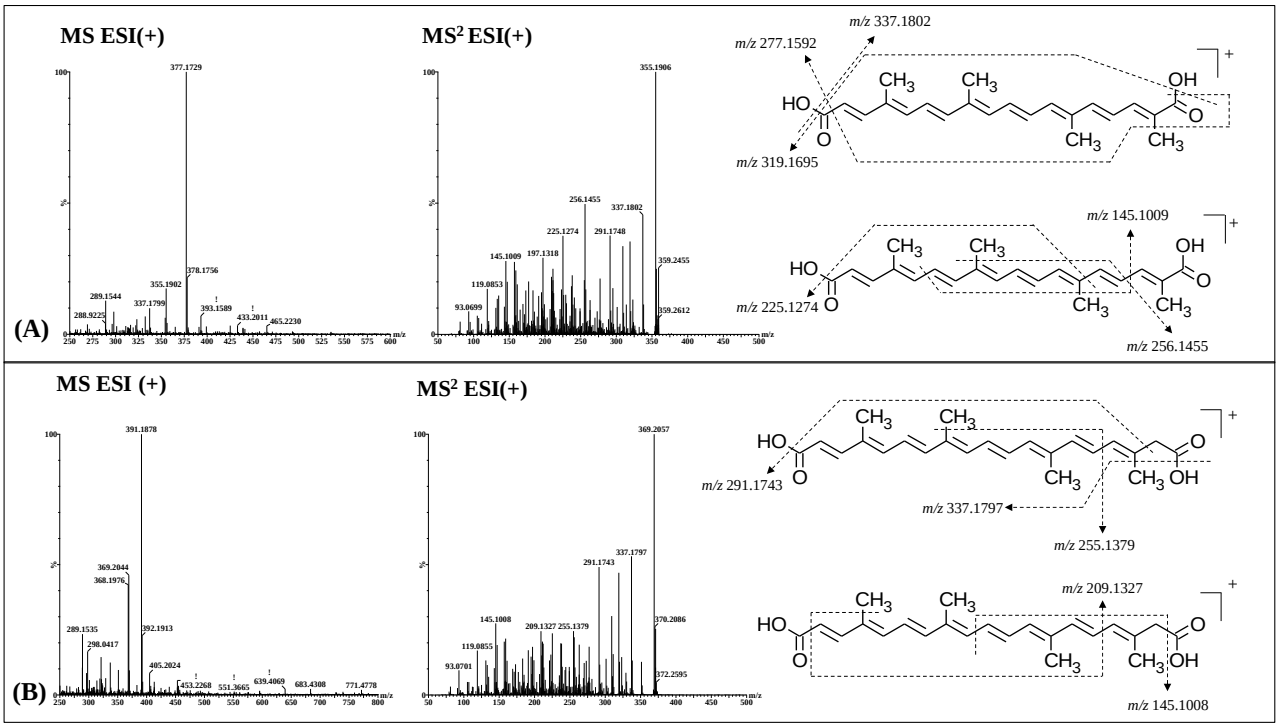

Fig. 4. Fragmentation study of compounds **2** (A) and **5** (B).

3.2. Purification and characterization of bixin

Analytical UPLC analysis at 460 nm showed 91% purity for the bixin isomer isolated from the Hex-Bo. Peak at 20.95 min showed λ_{max} at 430, 461 and 490 nm, with III/II band ratio of 33%, in accordance with previous studies (Chisté et al., 2011; Rios et al., 2007, 2005). In the positive ion mode, the $[M+H]^+$ molecular ion at *m/z* 395.2221 was dominant, and the MS/MS spectrum displayed fragments attributed to consecutive losses of H_2O (*m/z* 377.2103), CH_3OH (*m/z* 363.1950), CH_3OH + CO (*m/z* 335.1996) and CH_3OH + CO + H_2O (*m/z* 317.1903) (Fig. 5), all consistent with literature data (Chisté et al., 2011; Rehbein et al., 2007).

NMR experiments were performed in order to confirm the putative structure. In the olefinic region, ^{1}H NMR spectra showed signals at δ_H 7.88 (1H, d, J = 15.5 Hz, H-8'), δ_H 7.26 (1H, d, J = 15.5 Hz, H-8), δ_H 5.94 (1H, d, J = 15.5 Hz, H-7') and δ_H 5.82 (1H, d, J = 15.5 Hz, H-7) along with overlapped resonances integrating for ten protons at δ_H 6.40-6.95. A singlet integrating for three protons at δ_H 3.79 was attributed to the methyl ester protons. In addition, singlets at δ_H 1.89-1.97 accounted for the protons of the methyl groups linked to the polyunsaturated chain. In comparison with all-*E*-bixin or all *Z*-bixin, the disruption of the symmetry in the NMR shifts is due to the influence of a single *Z* double bond in Δ9'-10', and to the presence of a methyl ester group in 7', instead of a carboxylic acid in position 7.

(Rehbein et al., 2007). The correlations observed in the ^{1}H-^{1}H COSY spectrum confirm the unequivocal assignment of the signals H-7/H-8 and H-7'/H-8'(Fig. 5). H-8', neighboring the methyl ester group, is slightly more deshielded than H-8 neighboring the acid function. Previous chemical studies have also shown that the 9'-*Z*-bixin isomer is the most abundant in annatto seeds (Raddatz-Mota et al., 2017; Rivera-Madrid et al., 2016; Rodrigues et al., 2014; Tibodeau et al., 2010; Vilar et al., 2014), corroborating our results.

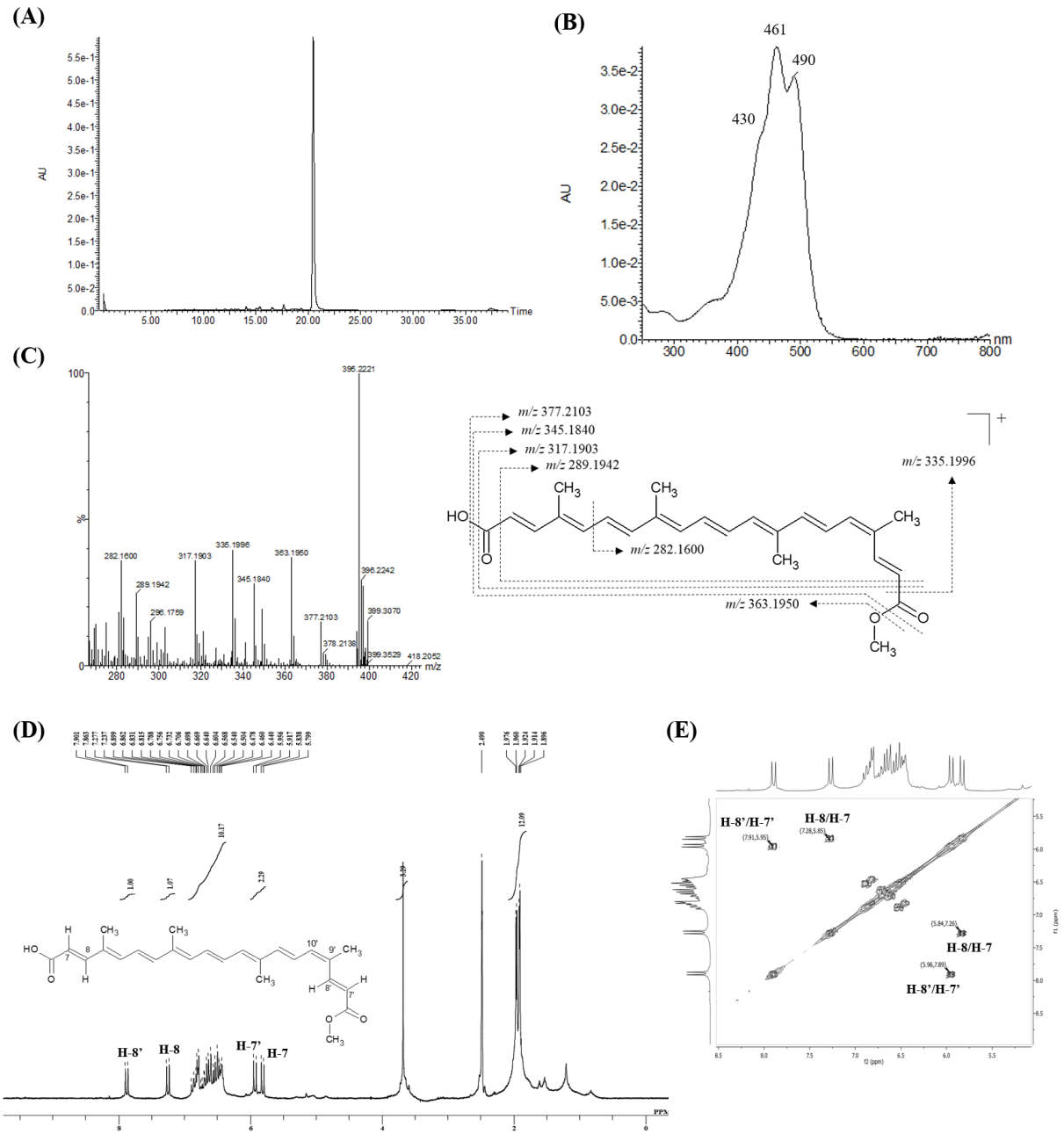

Fig. 5. UPLC-DAD chromatogram (A), UV spectrum (B), MS^{2}-ESI spectrum in positive mode ionization (C), ^{1}H NMR (D) and ^{1}H-^{1}H COSY (E) spectra of 9'-*Z*-bixin (bixin) purified from *B. orellana*.

3.3. Exposure to bixin inhibits proliferation and migration of A2058 cells

The intrinsic antiproliferative effect of bixin was determined by the MTT assay. Bixin promoted concentration-dependent cell growth inhibition, whose IC_{50} was determined as 40 µM (Fig. 6). In the cell migration assay, exposure to bixin (50 and 100 µM) suppressed cell migration into the zone free of cells (Fig. 6B). The migration rate decreased approximately in 55 and 72%, respectively, compared to the control group. These results suggest that bixin inhibits both proliferation and cell mobility.

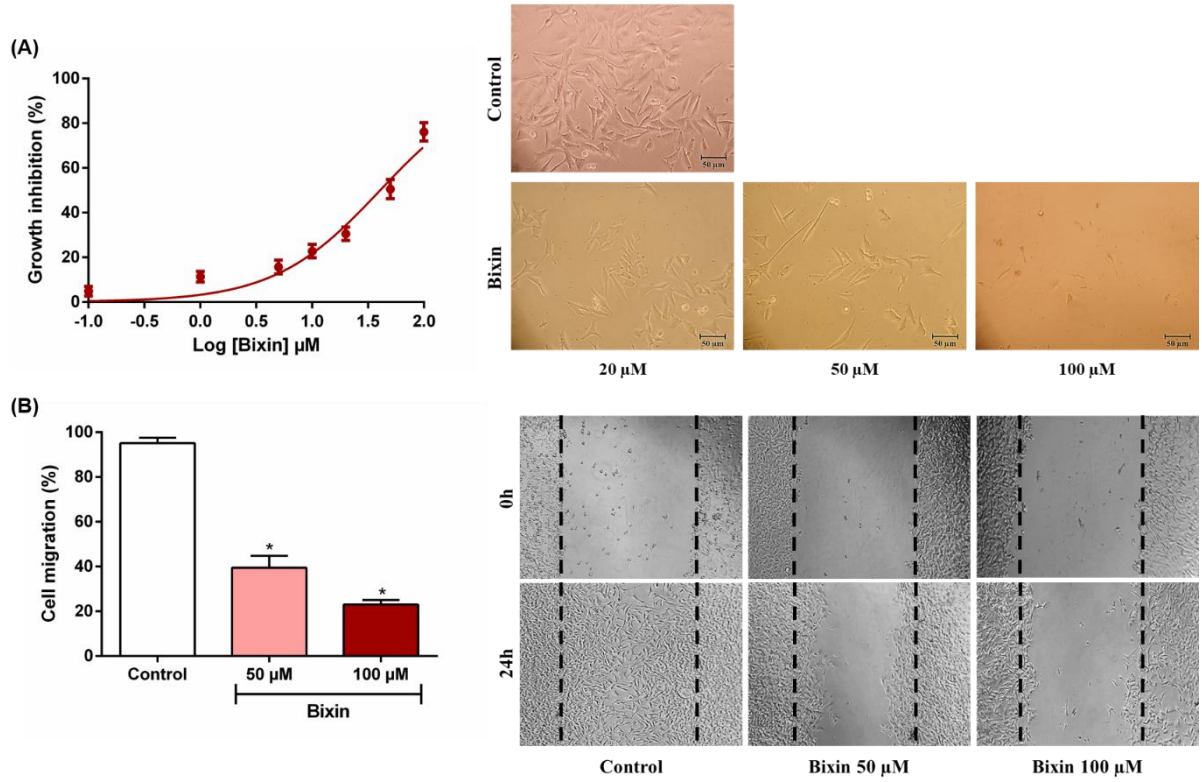

Fig. 6. Effect of bixin (0.1-100 µM) on cell viability (A) and cell migration (B). Photomicrographs represent the reduction of cell population (A) and cell migration into the zone free of cells (B) according to the treatment. Data are expressed as mean ± SEM, *p<0.05 (ANOVA one-way followed by Tukey's post-test).

3.4. Bixin potentiates antiproliferative and antimigratory activities of dacarbazine

To assess the capacity of bixin to potentiate the antiproliferative effect of market-available anticancer agents, A2058 cells were treated for 72h with bixin, vemurafenib and dacarbazine. Combined treatments were applied in order to compare them to the respective monotherapy. Vemurafenib is a BRAF inhibitor widely used in the treatment of metastatic

melanoma, whereas dacarbazine is an anticancer drug commonly used in combination with other chemotherapeutic agents (e.g. vemurafenib). As shown in Table 3, A2058 cells were sensitive to vemurafenib (IC_{50} = 6.96 µM), but resistant to dacarbazine therapy (IC_{50} > 100 µM).

Table 3. Antiproliferative activity of bixin and combined therapy (bixin + anticancer drugs) against A2058 cells. Data are presented as IC_{50} values and 95% confidence interval.

Monotherapy	IC_{50} (µM)	Combined therapy	IC_{50} (µM)
Bixin	40.53 (34.11 – 48.17)	-	-
Vemurafenib	6.96 (5.87 – 8.24)	Vemurafenib + Bixin	8.03 (7.09 – 9.08)
Dacarbazine	>>100	Dacarbazine + Bixin	31.85 (23.90 – 42.45)

Bixin was not able to potentiate the antiproliferative effect of vemurafenib (Fig. 7). However, melanoma cells were sensitive to dacarbazine when combined to bixin, exhibiting IC_{50} = 31.85 µM. Compared to the monotherapy, combined treatment induced a significant reduction in cell density (Fig. 7D). Control A2058 cells showed a regular epithelial morphology and became sub-confluent in 72h, while treated cells exhibited cell shrinkage and appearance of apoptotic cells.

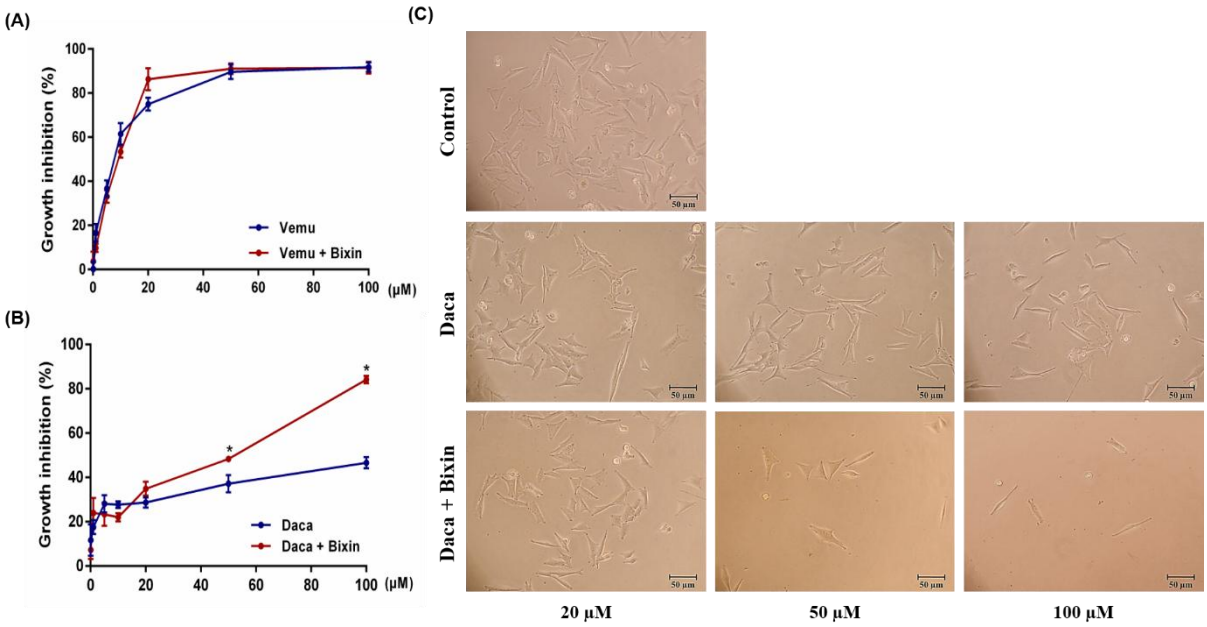

Fig. 7. Antiproliferative activity of bixin combined to vemurafenib (vemu) (A) and dacarbazine (daca) (B) in the MTT assay. Photomicrographs show reduction of cell population and cell shrinkage promoted by dacarbazine and bixin + dacarbazine treatments (C). Data are expressed as mean ± SEM, *p<0.05 according to unpaired Student's *t*.

Although A2058 cells have been shown to be resistant to dacarbazine therapy in the MTT assay, a significant reduction in cell migration was observed after 24h treatment with dacarbazine 50 and 100 μM. In addition, combined treatment (dacarbazine + bixin) presented a more intense pharmacological response when compared to monotherapy, suggesting that bixin also enhances the antimigratory potential of dacarbazine (Fig. 8).

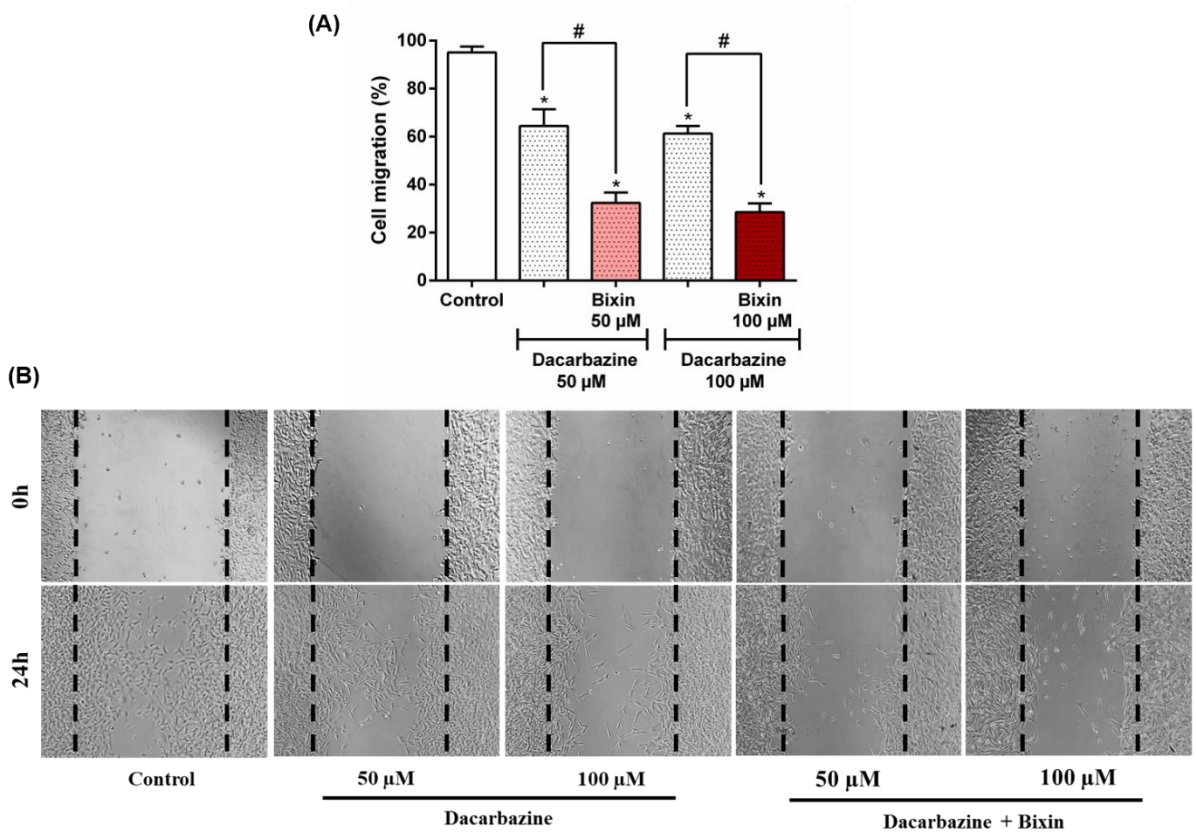

Fig. 8. Bixin enhances antimigratory effect of dacarbazine (A). Photomicrographs represent cell migration into the zone free of cells according to the treatment (B). Data are expressed as mean ± SEM, *p<0.05 (*vs* control group) and #p<0.05 (*vs.* dacarbazine), according to ANOVA one-way followed by Tukey's post-test.

3.5. Bixin enhances pro-apoptotic effect of dacarbazine

The pro-apoptotic effect of bixin and combined therapy was determined by double fluorescence staining with Annexin V and 6-CFDA, and by measuring the caspase-3 activity. 6-CFDA is used to measure cell viability, while Annexin V is a classic marker of phosphatidylserine externalization, a typical phenomenon for apoptotic cells. In this sense, living cells will only stain with 6-CFDA (green), cells in early apoptosis will stain both with Annexin V (red) and 6-CFDA, and cells in late apoptosis will stain with Annexin V and DAPI (blue). As shown in Fig. 9, bixin 50 µM increased the number of Annexin V and 6-CFDA double-stained cells, and Annexin V and DAPI stained cells, compared to control, suggesting that bixin presents significant pro-apoptotic activity. Dacarbazine 50 µM treatment also increased the number of cells in early apoptosis, but its pro-apoptotic effect was significantly improved when associated with bixin (Fig. 9A). Moreover, caspase-3 activity was significantly higher ($p<0.05$) in cells treated with combined therapy compared to treatments with dacarbazine or bixin (Fig. 9B). Caspase-3 is one of the most important pro-apoptotic enzymes, which can be activated by both intrinsic (mitochondrial) and extrinsic (death ligand) apoptosis pathways.

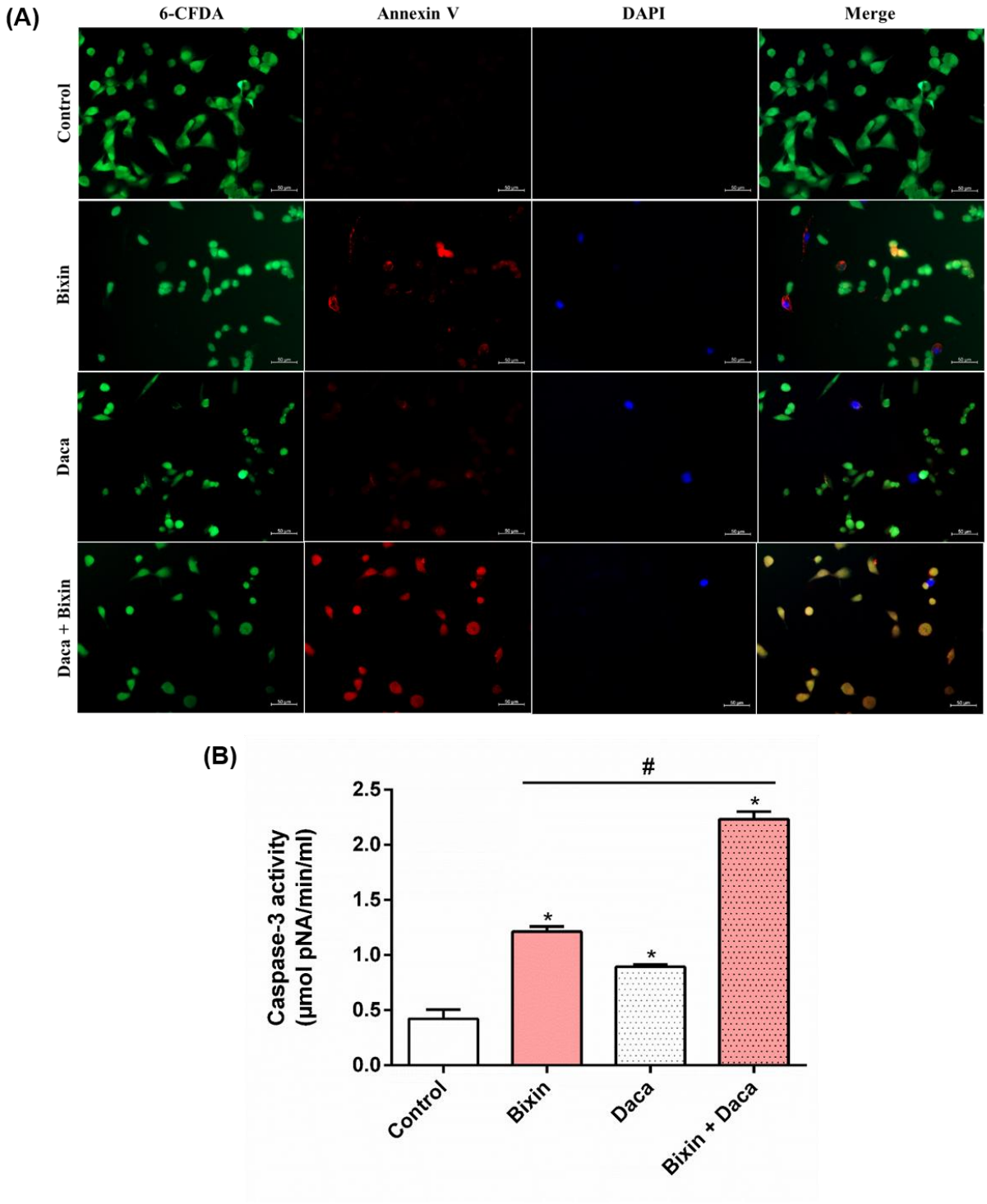

Fig. 9. Bixin improves pro-apoptotic effect of dacarbazine. Fluorescent micrographs show A2058 cells after Annexin V (red), 6-CFDA (green) and DAPI (blue) staining (A). Caspase-3 activity was evaluated after 72h of treatment (B). Cells were treated with bixin 50 µM, dacarbazine 50 µM (daca) or combined therapy (bixin + daca). Data are expressed as mean ± SEM, *$p<0.05$ (*vs.* control group) and $^{\#}p<0.05$ (*vs.* dacarbazine), according to ANOVA one-way followed by Tukey's post-test.

3.6. Bixin increases oxidative stress in combined treatment with dacarbazine

Although carotenoids are widely known for their antioxidant potential, a dual anti/pro-oxidant activity can also be observed for the same molecules. In fact, carotenoids exhibit high reactivity due to their conjugated double bonds system, which allows them to be readily oxidized by reactive oxygen species (ROS). In regular or high amounts of ROS, they are rapidly autoxidized and exhibit an expressive pro-oxidant activity. Pro-oxidant effects have also been reported when high concentrations of carotenoids were used. In cancer cells, these effects may induce oxidative damage to DNA, cell membrane and proteins involved in cell survival, inhibiting tumor growth (Eghbaliferiz and Iranshahi, 2016; Nagao, 2004; Ribeiro et al., 2018). As previously reported, bixin has anti and pro-oxidant potential based on the tested concentrations and other biochemical factors (Anantharaman et al., 2016; Mohan et al., 2018; Tay-agbozo et al., 2018). The pharmacological activities of bixin have been demonstrated mostly on carcinogenesis and lipid peroxidation (Anantharaman et al., 2016; Santos et al., 2016), but the involvement of its pro-oxidant effect in sensitizing tumor cells to chemotherapy has not been properly explored so far.

In this study, we investigated ROS and MDA levels in A2058 cells treated with bixin, dacarbazine and combined drugs. ROS generation was assessed 24h after treatments. Fluorescent micrographs of stained cells suggested that bixin 50 µM and dacarbazine 50 µM elevated ROS intensity compared to control cells. In addition, combined therapy (bixin + dacarbazine) exhibited higher ROS intensity than control and monotherapy conditions (Fig. 10A). Quantitative measurement of ROS level corroborated this result (Fig. 10B). ROS production was significantly increased ($p<0.05$) in cells treated with combined therapy compared to monotherapies. Similarly, combined therapy also increased MDA production compared to treatment with dacarbazine or bixin, suggesting cell membrane damage possibly caused by increased ROS production (Fig. 10C). Possible damage to the cell membrane could facilitate the entry of dacarbazine into the cell, justifying the enhancement of its pro-apoptotic effect during combined therapy.

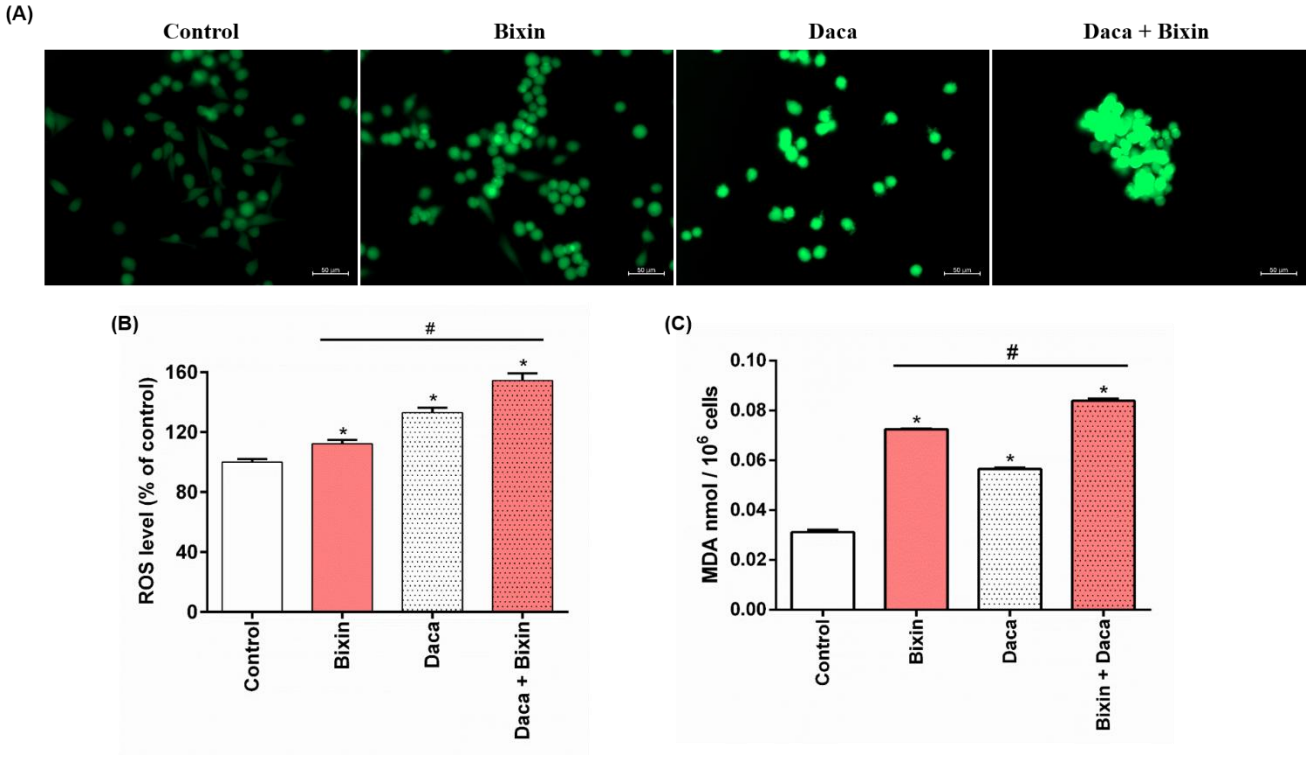

Fig. 10. Effect of bixin 50 µM, dacarbazine 50 µM (daca), and combined therapy (bixin + daca) on qualitative (A) and quantitative (B) ROS generation and MDA production (C) in A2058 cells. Data are expressed as mean ± SEM, $^{*}p<0.05$ (*vs.* control group) and $^{\#}p<0.05$ (*vs.* bixin and dacarbazine groups), according to ANOVA one-way followed by Tukey's post-test.

3.7. Cell cycle analysis

Evaluation of cell cycle progression by flow cytometry revealed an increase in G2/M cell population after treatment with bixin 50 µM (Fig. 11). Anantharaman et al. (2016) has also demonstrated that bixin induces cell cycle arrest in the G2/M phase in experiments performed with B16 murine melanoma cells. In addition, our results also showed an increase in sub-G1 (apoptotic) cells after exposure to dacarbazine 50 µM and combined therapy (dacarbazine + bixin) compared to untreated cells. However, no significant change between these groups was observed, indicating that bixin exerts no significant contribution on dacarbazine-induced cell cycle arrest.

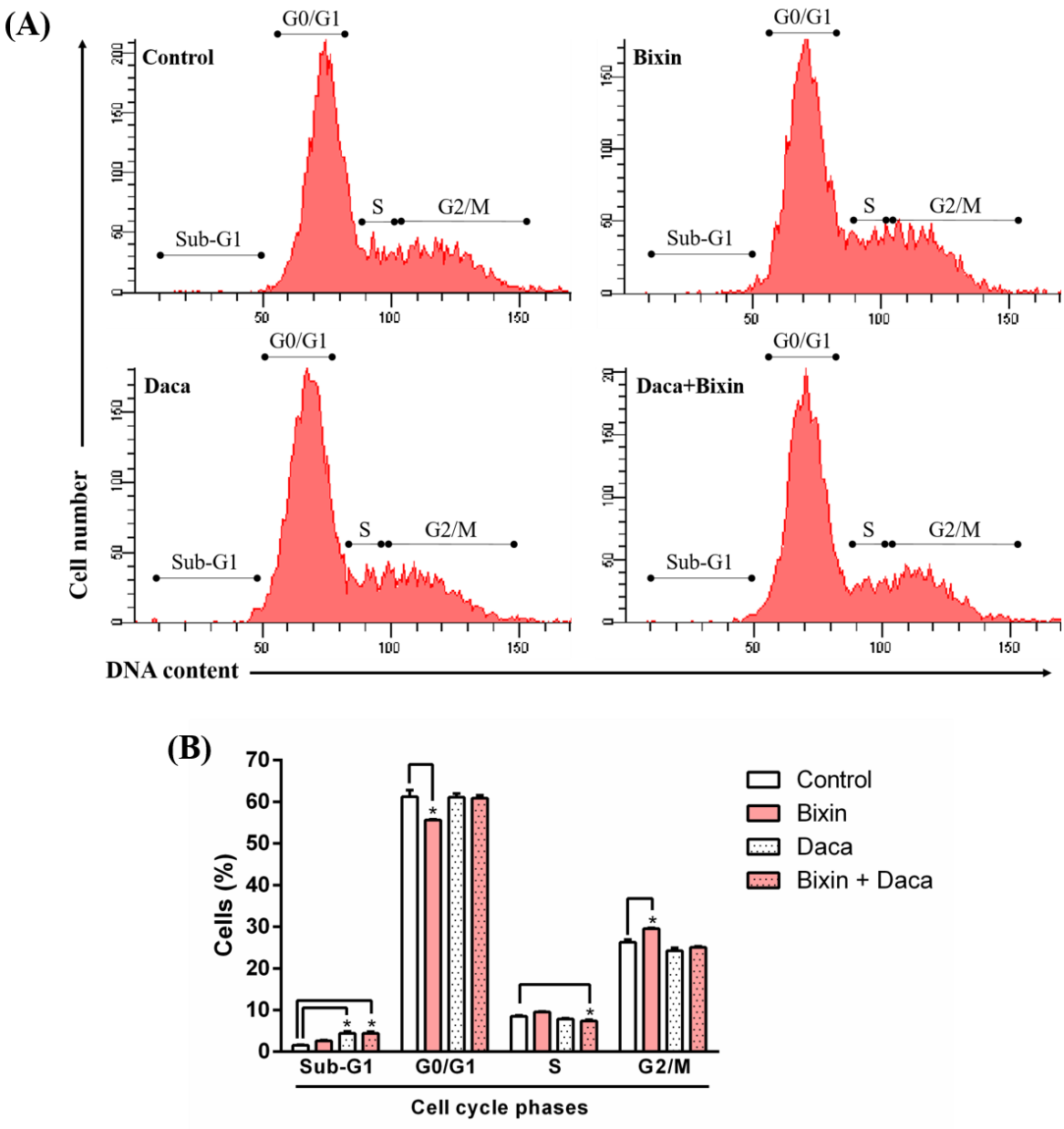

Fig. 11. Effect of bixin 50 µM, dacarbazine 50 µM (daca) and combined therapy (daca + bixin) on different phases of cell cycle. A2058 cells were treated for 72h, stained with propidium iodide and measured by flow cytometry, as shown in the representative histograms (A) and quantitative distribution of cells in different phases of cell cycle (B). Data are expressed as mean ± SEM, $^{*}p<0.05$ (*vs.* control group) according to ANOVA one-way followed by Tukey's post-test.

4. Conclusion

B. orellana bioactive extracts were chemically characterized by UPLC-DAD-MS/MS analysis, which led to the identification of two new apocarotenoids (compounds **2** and **5**). After being detected as a major component, 9'-*Z*-bixin was purified and tested in viability and

cell migration models. *In vitro* assays showed that bixin restored the sensitivity of A2058 melanoma cells to dacarbazine and enhanced its antimigratory activity. Different experiments also indicated that this apocarotenoid potentiated the pro-apoptotic effect of dacarbazine by increasing oxidative stress. Further investigations will be mandatory to confirm the pharmacological interest of bixin to potentiate the antitumour activity of antimelanoma drugs in *in vivo* models.

Conflicts of interest

There are no conflict of interest to declare.

Acknowledgements

This study was supported by the French cancer league (Comité 17 de la Ligue Nationale contre le Cancer).

Abbreviations

Daca (dacarbazine)
MDA (malondialdehyde)
MDR (multidrug resistance)
MTT (3-(4,5-dimethyl-2-thiazolyl)-2,5-diphenyl-2-H-tetrazolium bromide)
ROS (reactive oxygen species)

References

Agner, A.R., Barbisan, L.F., Scolastici, C., Salvadori, D.M.F., 2004. Absence of carcinogenic and anticarcinogenic effects of annatto in the rat liver medium-term assay. Food Chem. Toxicol. 42, 1687–1693. https://doi.org/10.1016/j.fct.2004.06.005

Ahamad, M.S., Siddiqui, S., Jafri, A., Ahmad, S., Afzal, M., Arshad, M., 2014. Induction of apoptosis and antiproliferative activity of naringenin in human epidermoid carcinoma cell through ROS generation and cell cycle arrest. PLoS One 9. https://doi.org/10.1371/journal.pone.0110003

Anantharaman, A., Hemachandran, H., Mohan, S., Manikoth Ayyathan, D., Kumar, D.T., George Priya Doss, C., Siva, R., 2016. Induction of apoptosis by apocarotenoids in B16 melanoma cells through ROS-mediated mitochondrial-dependent pathway. J. Funct. Foods 20, 346–357. https://doi.org/10.1016/j.jff.2015.11.019

Bautista, A.R.P.L., Moreira, E.L.T., Batista, M.S., Miranda, M.S., Gomes, I.C.S., 2004.

Subacute toxicity assessment of annatto in rat. Food Chem. Toxicol. 42, 625–629. https://doi.org/10.1016/j.fct.2003.11.007

Bhatia, S., Tykodi, S.S., Thompson, J.A., 2009. Treatment of metastatic melanoma: an overview. Oncology (Williston Park). 23, 488–96.

Chakraborty, R., Wieland, C.N., Comfere, N.I., 2013. Molecular targeted therapies in metastatic melanoma. Pharmgenomics. Pers. Med. 6, 49–56. https://doi.org/10.2147/PGPM.S44800

Chapman, P.B., Hauschild, A., Robert, C., Haanen, J.B., Ascierto, P., Larkin, J., Dummer, R., 2011. Improved survival with vemurafenic in melanoma with BRAF V600E mutation. N Eng J Med 364, 2507–2516. https://doi.org/10.1056/NEJMoa1103782.Improved

Chisté, R.C., Yamashita, F., Gozzo, F.C., Mercadante, A.Z., 2011. Simultaneous extraction and analysis by high performance liquid chromatography coupled to diode array and mass spectrometric detectors of bixin and phenolic compounds from annatto seeds. J. Chromatogr. A 1218, 57–63. https://doi.org/10.1016/j.chroma.2010.10.094

Cisilotto, J., Sandjo, L.P., Faqueti, L.G., Fernandes, H., Joppi, D., Biavatti, M.W., Creczynski-Pasa, T.B., 2018. Cytotoxicity mechanisms in melanoma cells and UPLC-QTOF/MS2chemical characterization of two Brazilian stingless bee propolis: Uncommon presence of piperidinic alkaloids. J. Pharm. Biomed. Anal. 149, 502–511. https://doi.org/10.1016/j.jpba.2017.11.038

Dankort, D., Curley, D.P., Cartlidge, R.A., Nelson, B., Karnezis, A.N., Damsky Jr, W.E., You, M.J., DePinho, R.A., McMahon, M., Bosenberg, M., 2009. BrafV600E cooperates with Pten loss to induce metastatic melanoma. Nat. Genet. 41, 544–552. https://doi.org/10.1038/ng.356

de Oliveira Júnior, R.G., Christiane Adrielly, A.F., da Silva Almeida, J.R.G., Grougnet, R., Thiéry, V., Picot, L., 2018. Sensitization of tumor cells to chemotherapy by natural products: A systematic review of preclinical data and molecular mechanisms. Fitoterapia 129, 383–400. https://doi.org/10.1016/j.fitote.2018.02.025

Eghbaliferiz, S., Iranshahi, M., 2016. Prooxidant Activity of Polyphenols, Flavonoids, Anthocyanins and Carotenoids: Updated Review of Mechanisms and Catalyzing Metals. Phyther. Res. 1391, 1379–1391. https://doi.org/10.1002/ptr.5643

Flaherty, K.T., McArthur, G., 2010. BRAF, a target in melanoma. Cancer 116, 4902–4913. https://doi.org/10.1002/cncr.25261

Garbe, C., Radny, P., Linse, R., Dummer, R., Gutzmer, R., Ulrich, J., Stadler, R., Weichenthal, M., Eigentler, T.K., Ellwanger, U., Hauschild, A., 2008. Adjuvant low-

dose interferon α2a with or without dacarbazine compared with surgery alone: A prospective-randomized phase III DeCOG trial in melanoma patients with regional lymph node metastasis. Ann. Oncol. 19, 1195–1201. https://doi.org/10.1093/annonc/mdn001

Grotto, D., Santa Maria, L., Valentini, J., Paniz, C., Schmitt, G., Garcia, S.C., Pomblum, V.J., Rocha, J.B.T., Farina, M., 2009. Importance of the lipid peroxidation biomarkers and methodological aspects for malondialdehyde quantification. Quim. Nova 32, 169–174. https://doi.org/10.1590/S0100-40422009000100032

Jin, S., Mishra-kalyani, P.S., Sridhara, R., 2018. Unresectable and Metastatic Melanoma of the Skin : Literature Review of Clinical Trials and Efficacy Endpoints Since 2000. https://doi.org/10.1177/2168479018769286

Jondiko, I.J.O., Pattenden, G., 1989. Terpenoids and an apocarotenoid from seeds of Bixa orellana. Phytochemistry 28, 3159–3162. https://doi.org/10.1016/0031-9422(89)80298-5

Juin, C., Oliveira Junior, R.G. de, Fleury, A., Oudinet, C., Pytowski, L., Bérard, J.B., Nicolau, E., Thiéry, V., Lanneluc, I., Beaugeard, L., Prunier, G., Almeida, J.R.G.D.S., Picot, L., 2018. Zeaxanthin from Porphyridium purpureum induces apoptosis in human melanoma cells expressing the oncogenic BRAF V600E mutation and sensitizes them to the BRAF inhibitor vemurafenib. Brazilian J. Pharmacogn. 28, 457–467. https://doi.org/10.1016/j.bjp.2018.05.009

Locatelli, C., Filippin-monteiro, F.B., Creczynski-pasa, T.B., 2013. Current Therapies and New Pharmacologic Targets for Metastatic Melanoma. Recent Adv. Biol. Ther. Manag. Melanoma. https://doi.org/10.5772/46052

MacKie, R.M., Hauschild, A., Eggermont, A.M.M., 2009. Epidemiology of invasive cutaneous melanoma. Ann. Oncol. 20, vi1-vi7. https://doi.org/10.1093/annonc/mdp252

Mercadante, A.Z., Steck, A., Pfander, H., 1997. Isolation and structure elucidation of minor carotenoids from annatto (Bixa orellana L.) seeds. Phytochemistry 46, 1379–1383. https://doi.org/10.1016/S0031-9422(97)00462-7

Mohan, S., Rajendra, P., Hemachandran, H., Kumar, P., 2018. Prospects and progress in the production of valuable carotenoids : Insights from metabolic engineering , synthetic biology , and computational approaches 266, 89–101. https://doi.org/10.1016/j.jbiotec.2017.12.010

Mosmann, T., 1983. Rapid colorimetric assay for cellular growth and survival: Application to proliferation and cytotoxicity assays. J. Immunol. Methods 65, 55–63. https://doi.org/10.1016/0022-1759(83)90303-4

Mouawad, R., Sebert, M., Michels, J., Bloch, J., Spano, J.P., Khayat, D., 2010. Treatment for metastatic malignant melanoma: Old drugs and new strategies. Crit. Rev. Oncol. Hematol. 74, 27–39. https://doi.org/10.1016/j.critrevonc.2009.08.005

Nagao, A., 2004. Functions and Actions of Retinoids and Carotenoids : Building on the Vision of James Allen Olson Carotene Oxygenases : A New Family of Double Bond Cleavage Enzymes. Am. Soc. Nutr. Sci. 246–250.

Paumgartten, F.J.R., De-Carvalho, R.R., Araujo, I.B., Pinto, F.M., Borges, O.O., Souza, C.A.M., Kuriyama, S.N., 2002. Evaluation of the developmental toxicity of annatto in the rat. Food Chem. Toxicol. 40, 1595–1601. https://doi.org/10.1016/S0278-6915(02)00133-3

Priya, R., Sneha, P., Madrid, R.R., C, G.P.D., 2017. Molecular Modeling and Dynamic Simulation of Arabidopsis Thaliana Carotenoid Cleavage Dioxygenase Gene: A Comparison with Bixa orellana and Crocus Sativus 2721, 2712–2721. https://doi.org/10.1002/jcb.25919

Raddatz-Mota, D., Pérez-Flores, L.J., Carrari, F., Mendoza-Espinoza, J.A., de León-Sánchez, F.D., Pinzón-López, L.L., Godoy-Hernández, G., Rivera-Cabrera, F., 2017. Achiote (Bixa orellana L.): a natural source of pigment and vitamin E. J. Food Sci. Technol. 54, 1729–1741. https://doi.org/10.1007/s13197-017-2579-7

Rehbein, J., Dietrich, B., Grynbaum, M.D., Hentschel, P., Holtin, K., Kuehnle, M., Schuler, P., Bayer, M., Albert, K., 2007. Characterization of bixin by LC-MS and LC-NMR. J. Sep. Sci. 30, 2382–2390. https://doi.org/10.1002/jssc.200700089

Ribeiro, D., Freitas, M., Silva, A.M.S., Carvalho, F., Fernandes, E., 2018. Antioxidant and pro-oxidant activities of carotenoids and their oxidation products. Food Chem. Toxicol. 120, 681–699. https://doi.org/10.1016/j.fct.2018.07.060

Rios, A. de O., Mercadante, A.Z., Borsarelli, C.D., 2007. Triplet state energy of the carotenoid bixin determined by photoacoustic calorimetry. Dye. Pigment. 74, 561–565. https://doi.org/10.1016/j.dyepig.2006.03.018

Rios, A.D.O., Borsarelli, C.D., Mercadante, A.Z., 2005. Thermal degradation kinetics of bixin in an aqueous model system. J. Agric. Food Chem. 53, 2307–2311. https://doi.org/10.1021/jf0481655

Rivera-Madrid, R., Aguilar-Espinosa, M., Cárdenas-Conejo, Y., Garza-Caligaris, L.E., 2016. Carotenoid Derivates in Achiote (Bixa orellana) Seeds: Synthesis and Health Promoting Properties. Front. Plant Sci. 7, 1–7. https://doi.org/10.3389/fpls.2016.01406

Rodrigues, L.M., Alcázar-Alay, S.C., Petenate, A.J., Meireles, M.A.A., 2014. Bixin extraction

from defatted annatto seeds. Comptes Rendus Chim. https://doi.org/10.1016/j.crci.2013.10.010

Santos, G., Almeida, M., Antunes, L., Bianchi, M., 2016. Effect of bixin on DNA damage and cell death induced by doxorubicin in HL60 cell line. Hum. Exp. Toxicol. 35, 1319–1327. https://doi.org/10.1177/0960327116630352

Shahid-ul-Islam, Rather, L.J., Mohammad, F., 2016. Phytochemistry, biological activities and potential of annatto in natural colorant production for industrial applications – A review. J. Adv. Res. 7, 499–514. https://doi.org/10.1016/j.jare.2015.11.002

Sosman, J.A., Puzanov, I., 2006. Molecular targets in melanoma from angiogenesis to apoptosis. Clin. Cancer Res. 12, 2376–2384. https://doi.org/10.1158/1078-0432.CCR-05-2558

Stohs, S.J., 2014. Safety and efficacy of Bixa orellana (achiote, annatto) leaf extracts. Phyther. Res. 28, 956–960. https://doi.org/10.1002/ptr.5088

Tay-agbozo, S., Street, S., Kispert, L., 2018. Journal of Photochemistry & Photobiology , B : Biology The carotenoid Bixin found to exhibit the highest measured carotenoid oxidation potential to date consistent with its practical protective use in cosmetics , drugs and food. J. Photochem. Photobiol. B Biol. 186, 1–8. https://doi.org/10.1016/j.jphotobiol.2018.06.016

Tentori, L., Lacal, P.M., Graziani, G., 2013. Challenging resistance mechanisms to therapies for metastatic melanoma. Trends Pharmacol. Sci. 34, 656–666. https://doi.org/10.1016/j.tips.2013.10.003

Tibodeau, J.D., Isham, C.R., Bible, K.C., 2010. Annatto constituent cis-bixin has selective antimyeloma effects mediated by oxidative stress and associated with inhibition of thioredoxin and thioredoxin reductase. Antioxid. Redox Signal. 13, 987–97. https://doi.org/10.1089/ars.2009.2896

Tocchini, L., Mercadante, A.Z., 2001. Extração E Determinação, Por Clae, De Bixina E Norbixina Em Colorí ficos. Ciência e Tecnol. Aliment. 21, 310–313. https://doi.org/10.1590/S0101-20612001000300010

Vilar, D. de A., Vilar, M.S. de A., de Lima e Moura, T.F.A., Raffin, F.N., de Oliveira, M.R., Franco, C.F. de O., de Athayde-Filho, P.F., Diniz, M. de F.F.M., Barbosa-Filho, J.M., 2014. Traditional uses, chemical constituents, and biological activities of Bixa orellana L.: a review. Sci. World J. 857292, 1–11. https://doi.org/10.1155/2014/857292

Vinod, B.S., Maliekal, T.T., Anto, R.J., 2013. Phytochemicals As Chemosensitizers: From Molecular Mechanism to Clinical Significance. Antioxid. Redox Signal. 18, 1307–1348.

https://doi.org/10.1089/ars.2012.4573

Graphical abstract